

**MOLECULAR SIMULATION STUDY OF POLYMER NANOCOMPOSITES
WITH HYDROGEN BONDING CHEMISTRIES**

by

Kevin J. Modica

A thesis submitted to the Faculty of the University of Delaware in partial fulfillment of the requirements for the degree of Honors Bachelor of Chemical Engineering with Distinction

Spring 2019

© 2019 Kevin J. Modica
All Rights Reserved

**MOLECULAR SIMULATION STUDY OF POLYMER NANOCOMPOSITES
WITH HYDROGEN BONDING CHEMISTRIES**

by

Kevin J. Modica

Approved: _____
Arthi Jayaraman, Ph.D.
Professor in charge of thesis on behalf of the Advisory Committee

Approved: _____
Eric Furst, Ph.D.
Committee member from the Department of Chemical and Biomolecular
Engineering

Approved: _____
Christopher Kloxin, Ph.D.
Committee member from the Board of Senior Thesis Readers

Approved: _____
Earl Lee II, Ph.D.
Deputy Faculty Director, University Honors Program

ACKNOWLEDGMENTS

I would like to thank my researcher advisor and mentor, Professor Arthi Jayaraman. Professor Jayaraman provided me with an opportunity to join her lab through the summer fellows program following my freshman year of college. In that summer and the continuing years, I have been lucky enough to work on incredible projects and publish two papers. Professor Jayaraman has been an outstanding role model as a passionate and thoughtful researcher, academic, and mentor. I am forever grateful for her guidance.

I would also like to thank Dr. Tyler Martin. When I first joined the Jayaraman group, I had taken one programming class, one chemical engineering class, and had exactly zero understanding of how to start on my project. Dr. Martin was always a friendly face and mentor who could push me in the right direction when I felt lost. Without his support, I cannot imagine being able to complete this thesis today.

I also want to thank the rest of the graduate students and postdoctoral researchers in the Jayaraman group. Their support and suggestions have been invaluable over the course of this thesis and my undergraduate career. I would like to specifically thank Thomas Gartner and Arjita Kulshreshtha. Tom has been so patient when listening to my questions, concerns, and ideas. Without Tom's example and guidance, I would not have understood what to look for in a graduate school or in a career. I would like to thank Arjita for her mentorship and assistance in writing this thesis as well as the opportunity to learn from her as we worked on writing our paper together.

Outside of the Jayaraman group, there are so many people at UD that I am grateful for. I want to thank everyone in the Chemical Engineering department that has helped me along the way to graduation, especially to Professor Josh Enszer and Professor Abraham Lenhoff.

Lastly, I want to thank my incredible friends and family for their support and companionship throughout this process. Special thank you to Phoebe, Stephen, Eleanor, Owen, Jacob, Caitlin, Tyler, and Vikki. Their friendship, help studying, and sense of humor kept me sane in the whirlwind that is college.

Most importantly, thank you to my mom, Danette, my dad, Joe, and my dog, Lucky, for being the best family I could ever ask for. You all have given me so much and I hope I make you proud.

TABLE OF CONTENTS

LIST OF TABLES	vi
LIST OF FIGURES	vii
ABSTRACT	viii
1 INTRODUCTION AND MODEL DEVELOPMENT	1
1.1 Background.....	1
1.2 Computational Approach.....	4
1.2.1 Model.....	5
1.2.2 Simulation Method	7
1.3 Analyses	9
2 SIMULATION RESULTS AND DISCUSSION.....	12
2.1 Results for Low Grafting Density Simulations	12
2.2 CONCLUSIONS AND FUTURE WORK.....	19
REFERENCES	21
TEXT AND FIGURE REPRINT PERMISSION	25

LIST OF TABLES

Table 1: Quantification of grafted layer wetting for select systems, these results are for $D_P=5d$, $N_G=20$, $\Sigma =0.32$ chains/ d^2 and $N_M=20$	13
Table 2: Number of matrix chains interacting with each graft chain for the two cases of equivalent wetting. These results are for $D_P=5d$, $N_G=20$, $\Sigma =0.32$ chains/ d^2 and $N_M=20$	17

LIST OF FIGURES

Figure 1: Schematic of the CG model of the polymer grafted nanoparticle and matrix polymer in the absence of h-bonding sites (a) and with h-bonding sites (b) (not drawn to scale).	4
Figure 2: Schematic showing a) bonded potential parameters between backbone-backbone beads and backbone A-D beads b) angle potential parameters between consecutive backbone beads and A-D sites and backbone chains.	7
Figure 3: A simulation snapshot of a representative equilibrated structure showing a grafted particle with graft polymer chains in blue and one matrix chain in green. Other matrix chains are set to be partially transparent for ease of view of the polymer grafted nanoparticle in the center. The red and yellow sites are the acceptor and donor beads. This image is rendered using OVITO software. ²⁹	9
Figure 4 Graft (decreasing with distance from particle surface) and matrix (increasing with distance from particle surface) monomer concentration profiles for PNCs with isotropic graft-matrix interaction and repulsive A-D interaction and for PNCs with attractive A-D interaction. The dashed lines represent the brush height of the grafted layer. These results are for $D_P=5d$, $N_G=20$, $\Sigma =0.32$ chains/ d^2 and $N_M=20$. Error bars (calculated as standard deviation from three independent simulation runs) when not visible are smaller than marker size.....	12
Figure 5: Probability distribution of the end-end distances, $P(R_{ee})$ vs. R_{ee} for graft chains. These results are for $D_P=5d$, $N_G=20$, $\Sigma =0.32$ chains/ d^2 and $N_M=20$. Error bars (calculated as standard deviation from three independent simulation runs) when not visible are smaller than marker size.....	15
Figure 6: Probability distribution of free volume per graft chain for the two cases that show equivalent wetting in Figure 4 and equivalent end-end distances in Figure 5. These results are for $D_P=5d$, $N_G=20$, $\Sigma =0.32$ chains/ d^2 and $N_M=20$. Error bars (calculated as standard deviation from three independent simulation runs) when not visible are smaller than marker size.....	18

ABSTRACT

In this thesis, I present a new coarse-grained (CG) model used to capture directional and specific interactions (eg. hydrogen bonding) present between acceptor—donor sites on graft and matrix chains in polymer nanocomposites (PNCs). This CG model represents acceptor and donor sites partially embedded in graft and matrix monomer beads to create the effect of directionality and specificity needed to mimic hydrogen bonding interactions. Then, this CG model is used in molecular dynamics simulation studies to understand how these directional and specific interactions impact PNC structure. We quantify the structure of the PNC using several methods: the interpenetration of matrix chains into the grafted layer (known as grafted layer wetting) found via concentration profiles, chain conformations described using end to end distance calculations, and the free volume of polymer chains. In collaboration with graduate student Arjita Kulshreshtha and under direction of Professor Arthi Jayaraman, we have found that while equivalent grafted layer wetting can be achieved with directional acceptor-donor interactions and isotropic graft – matrix interactions, there is a distinct difference in local chain structure and free volume in the polymer nanocomposite due to each of these interactions.

Chapter 1

INTRODUCTION AND MODEL DEVELOPMENT

Parts of this thesis and several figures are adapted with permission from Kulshreshtha, A.; Modica, K. J.; Jayaraman, A.; *Macromolecules* 2019, 52, 2725-2735. Copyright 2019 American Chemical Society.¹

1.1 Background

Polymer nanocomposites are materials that consist of a polymer matrix mixed with some nanoscale filler (in this case nanoparticles). Macroscopic properties of polymer nanocomposites (PNCs) are linked to the morphology and the aggregation or dispersion of nanoparticles within the polymer matrix. This work has been inspired by past studies demonstrating that the PNC morphology can be tuned by grafting the nanoparticle surface with polymers. The architecture, flexibility, chemistries, and grafting density of these polymers then impact the dispersion and assembly of the particles present.²⁻⁶ Using these design parameters, one can also influence the extent of penetration of matrix chains into the grafted layer (grafted layer wetting). Together the wetting/dewetting and the particle dispersion/aggregation will alter the macroscopic properties of the PNC.

The focus of this thesis was heavily inspired by my previous work.⁷ In that work the effect of grafted polymer architecture (linear and comb) was explored on PNC structure. Comb and linear architectures represent different types of connectivities between monomer units or Kuhn segments. Changing the connectivity

of the polymers allows for large changes in the structure of the grafted layer and therefore the effective size of the particles. That work also looked at the effect of curvature on the grafted layer structure. In that paper, we focused on studying polymer grafted nanoparticles (PGPs) without any enthalpic attraction or repulsion (known as the purely entropic or athermal limit). Therefore, differences in polymer chemistries were not explored. While the athermal limit provides important information on the entropic driving forces, the enthalpic forces which influence aggregation and dispersion are important as well. Varying polymer chemistries is a commonly used method to promote particle aggregation and dispersion, so it is important to consider those when designing experiments.

To that end, previous simulation, theory, and experimental studies have looked at graft and matrix polymers with isotropic interactions that are commonly described by the Flory Huggins parameter χ .⁸ In this work, χ_{GM} represents the relative attraction between graft (G) and matrix (M) polymer segments. A negative χ_{GM} value indicates that there is a relative enthalpic attraction between graft and matrix polymers as compared to graft-graft or matrix-matrix interactions and vice versa for positive χ_{GM} . Advances in experimental synthesis and characterizations have allowed experimentalists to consider the role of graft-matrix hydrogen bonding (h-bonds) in creating thermally reversible materials with dispersion-aggregation transitions mediated by h-bonds.¹⁰

Previous studies on h-bonding interactions in carbon nanotube (CNT) nanocomposites have shown that improving the accessibility of h-bonding groups leads to enhanced dispersion of CNTs in a polymer matrix and improved mechanical and electrical properties.¹¹ Similarly, h-bonding interactions have been used to tune

miscibility in polymer blends¹²⁻¹⁴ and to create supramolecular assemblies of nanoparticles in matrix dependent on temperature¹⁵ and pH.¹⁶ These studies support the fact that PNCs with h-bonding interactions have a promising potential for programmable assembly and for fabrication of materials with unique properties such as self-healing and stimuli responsiveness attributed to the dynamic properties of h-bonds.

While experimental studies have demonstrated that h-bonds can enhance properties of polymer blends and nanocomposites,^{16,17} theory and simulation studies are needed to efficiently and economically explore the large design parameter space of PNCs with hydrogen bonding polymers. Therefore, I aim to use this CG model to study how the polymer morphology in PNCs can be tuned using h-bonding interactions, which would therefore alter macroscopic properties of the PNC.

Coarse-grained models are needed to capture the large length and time scales involved in h-bonding without the prohibitive computational cost of using atomistic models. It is especially important to capture the directionality and specificity of h-bonds in the CG model, as opposed to modelling is as isotropic attraction. CG models that capture these features have been created for biological systems. For example, a CG model for DNA has been developed by the Sciortino group^{18,19} which incorporates a “sticky-bead” to create a hydrogen bonding site. This model has been expanded by the Jayaraman group to mimic the specificity of h-bonding and match the melting trends of DNA oligomers and collagen-like-peptides (CLPs).²⁰⁻²²

In this thesis, a CG model based is used to capture h-bonding interactions between graft and matrix polymer chains in a polymer grafted nanoparticle PNC. This is also used to computationally predict how different enthalpic interactions (isotropic

interactions vs h-bonding attractions) influence the grafted layer wetting and local structure, which in turn affect nanoparticle aggregation or dispersion within the PNC.

The chapter is organized as follows. In Section 1.1, I have discussed the background and motivation for this thesis. In Section 1.2, I will go over the details of the model, simulation method, and methods of analyses.

1.2 Computational Approach

This section will discuss the computational approach used to simulate nanocomposites containing polymer grafted particles including the incorporation of the donor and acceptor sites used to capture the directional and specific interactions.

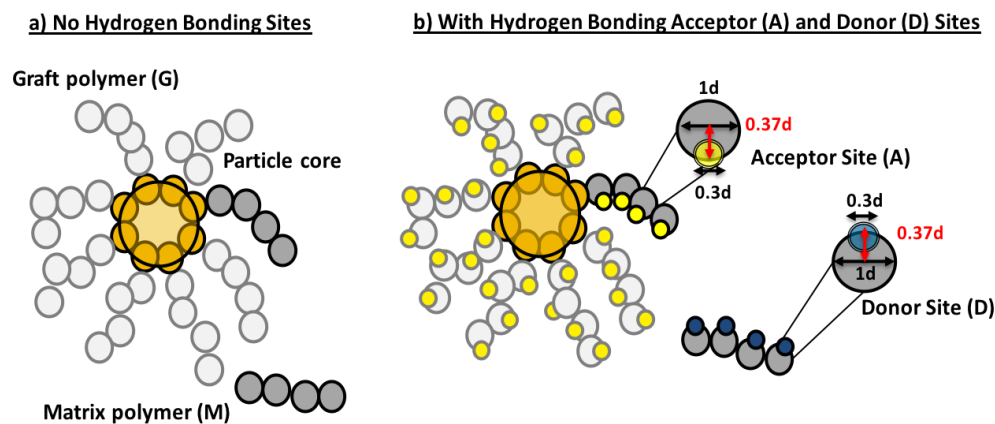


Figure 1: Schematic of the CG model of the polymer grafted nanoparticle and matrix polymer in the absence of h-bonding sites (a) and with h-bonding sites (b) (not drawn to scale).

1.2.1 Model

Figure 1 shows the CG model where the polymer grafted particle has a spherical nanoparticle core of diameter D_P , grafted with bead-spring²³ polymer chains with each CG bead of diameter d representing a monomer. The graft chains are attached to the nanoparticle core through harmonic bond potentials. Matrix chains are also modeled like the graft polymer chains. The bonded interactions include a harmonic spring between bonded CG monomers in the graft and matrix chains, as well as a harmonic angle potential between three bonded CG monomers whose force constant allows us to vary the graft and matrix chain flexibility in a manner similar to Lin et al.²⁴ The non-bonded interactions between pairs of graft (G) and matrix (M) monomers are modeled using Lennard Jones (LJ)²⁵ potential with $\sigma_{ij} = 1.0d$ and $r_{cut} = 2.0d$, and $\epsilon_{GG} = \epsilon_{MM} = 0.5kT$ and ϵ_{GM} varying from $0.2kT$ (to get $\chi_{GM} = +0.3$) to $1.0kT$ (to get $\chi_{GM} = -0.5$). For PNCs with h-bonding graft and matrix monomer chemistries, an acceptor bead (A) is placed on the graft bead and a donor bead (D) is placed on the matrix bead, as shown in Figure 1b, to act as intermolecular h-bonding sites between graft and matrix monomers. These A and D beads of size $0.3d$ are maintained at specific positions with respect to the G and M beads' centers via bonded harmonic interactions of force constant $k_{bond} = 1000 kT/d^2$ and an equilibrium bond distance $r_0 = 0.37d$. There are no A-G-G-A or D-M-M-D bonded dihedral potentials in this work, however, this can easily be introduced in our model to mimic torsional constraints imposed on the h-bonding donor and acceptor atoms in some graft and matrix chemistries.²⁶ The non-bonded A-D interaction is defined using LJ potential with $\sigma_{AD} = 0.3d$, $r_{cut} = 2 * \sigma_{AD}$, and $\epsilon_{AD} = 13kT$ to mimic the maximum strength of OH:N h-bond pair. I choose this specific pair of interactions to mimic polymer chemistries like the ones in the experimental studies by Hayward and coworkers

where they used poly(styrene-r-2-vinylpyridine) grafts in a poly(styrene-r-4-vinyl phenol) matrix and found improved particle dispersion mediated by h-bonds between graft and matrix polymers.¹⁰ All other pair-wise non-bonded interactions involving the nanoparticle, P, (i.e., A-P, D-P, G-P, and M-P), and involving graft, matrix, acceptors and donors (i.e., G-A, M-A, G-D, and M-D) are modeled as purely repulsive using Weeks Chandler Andersen²⁷ (WCA) potential.

The directionality of A-D interactions is brought about by the relative size and placement of A and D beads with respect to their attached G and M beads' center, as shown in Figure 2a. The specificity of the h-bonding interaction (i.e., preference for A-D over A-A and D-D and preventing possibility of A-D-A or A-D-D interactions) is brought about by A-A and D-D repulsive interactions modeled using WCA potential with $\sigma_{AA} = \sigma_{DD} = 2.3 * \sigma_{AD}$ and $r_{cut} = 1.1225 * \sigma_{AA}$ and $\epsilon_{AA} = \epsilon_{DD} = 0.5kT$. This repulsive potential ensures that a D or A site sees no energetically favorable patch as it approaches another pair of A and D sites that are close to each other and interacting via A-D attraction.

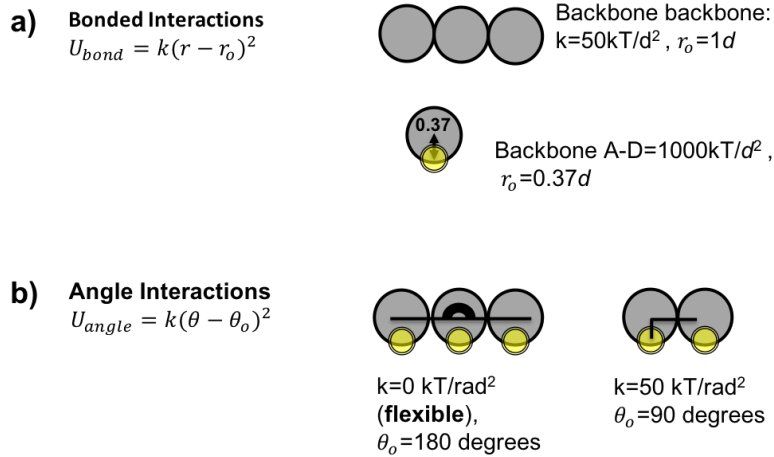


Figure 2: Schematic showing a) bonded potential parameters between backbone-backbone beads and backbone A-D beads b) angle potential parameters between consecutive backbone beads and A-D sites and backbone chains.

1.2.2 Simulation Method

The above CG model is used in a molecular dynamics (MD) simulation within LAMMPS package²⁸ using a protocol similar to previous work done by Jayaraman and coworkers.⁸ In this thesis, simulations are conducted for PNCs with a single polymer grafted nanoparticle with diameter $D_P = 5d$, graft chain length $N_g = 20$, grafting density $\Sigma = 0.32$ chains/ d^2 placed within a matrix with chain lengths of $N_M = 20$. The grafting density $\Sigma = 0.32$ chains/ d^2 mimic the intermediate grafting density and is selected to show the effects of h-bonding in this density of grafted chain conformations. The matrix chain length of 20 was chosen to study the case where the graft and matrix chain lengths are equal; a condition that is shown to be favorable for grafted layer wetting in the entropically driven limit. The total volume packing fraction, η , quantifies the fraction of the simulation box volume that is occupied by particle, graft and matrix beads and is maintained in this thesis at $\eta=0.367$; this value was chosen to achieve melt like conditions in a PNC. Since I simulate a single

polymer grafted particle within the polymer matrix, the grafted filler fraction defined as $\phi_G = \frac{V_{graft}+V_{particle}}{V_{graft}+V_{particle}+V_{matrix}}$ is kept at 0.01 where V_{graft} , V_{matrix} , $V_{particle}$ represent the total volume occupied by graft, particle and matrix beads, respectively. A minimum box size is chosen to be 44d to eliminate any finite size effects.

To obtain an initial configuration for the simulations, I first create a polymer grafted particle of size $D_P=5d$ whose surface is tessellated by grafting site beads of size 1d. For $D_P=5d$, 25 grafting site beads were used for a grafting density of $0.32 \text{ chains}/d^2$. Graft polymer chains are attached to the grafting site beads through harmonic bonds. To ensure relaxation of graft chains from the chosen initial configuration, a single polymer grafted particle (without any matrix chains) keeping all interactions (graft-graft, acceptor-acceptor, acceptor-graft, acceptor-particle and graft-particle) as purely repulsive, specified by WCA potential, over 1 million time steps where each time step $=0.001 * \sigma(m/\epsilon)^{0.5}$. Then, the equilibrated polymer grafted particle is placed at the center of the simulation box and the matrix chains of length N_M are added into the simulation box volume that is 50 times larger than the actual simulation box used for the production run. A larger box size helps accommodate matrix chains around the polymer grafted particle without significant overlaps. Temperature is controlled using a Langevin thermostat with a damping parameter of 10τ for PNCs with time integration performed using the velocity Verlet algorithm. After the initial configuration relaxation of graft and matrix chains, the simulation box is gradually compressed over 2 million time steps to the desired box size to achieve $\eta = 0.376$. This final system size is equilibrated in NVT ensemble at $T^*=1$ for at least another 5 million time steps.

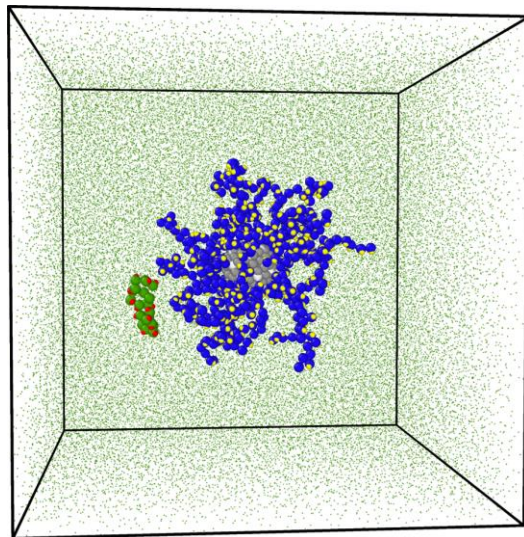


Figure 3: A simulation snapshot of a representative equilibrated structure showing a grafted particle with graft polymer chains in blue and one matrix chain in green. Other matrix chains are set to be partially transparent for ease of view of the polymer grafted nanoparticle in the center. The red and yellow sites are the acceptor and donor beads. This image is rendered using OVITO software.²⁹

The equilibrated system (as shown in Figure 3) is then used as a starting point to generate production run configurations which are saved every 0.1 million time steps and used for calculating ensemble averaged concentration profiles and performing other structural analysis.

1.3 Analyses

To quantify wetting and interpenetration between graft chains (G) and matrix chains (M) the monomer concentration profiles of graft (C_G) and matrix (C_M) chains²⁴ were plotted as a function of distance from the particle surface. C_x ($x = G$ or M) is given by:

$$C_x = \frac{\langle n_x(r) \rangle}{4\pi r^2 \Delta r} \quad (1)$$

where $\langle n_x(r) \rangle$ is the ensemble average number of monomers of type x within a shell of thickness $\Delta r=1d$ at a distance r from the particle surface. Error bars in all calculated quantities are from the standard deviation in average values from three independent simulation runs.

The effective thickness of grafted layer is represented by brush height which is calculated as the root mean square of the distance of the grafted beads from the particle surface.

$$H_B = \sqrt{\frac{\sum_1^{n_G} r_i^2}{n_G}} \quad (2)$$

where H_b is the brush height, r_i is the distance of grafted bead i from the particle surface and n_G is the total number of graft beads in the polymer grafted nanoparticle.

I calculate the number of matrix chains that interact with each graft chain by tracking the matrix chains whose beads lie in the interaction region (defined by potential cutoffs) for both isotropic G-M interaction and directional A-D interaction. I also calculate the average number of matrix beads within the grafted layer thickness as an additional method to quantify the extent of grafted layer wetting.

The conformations of the graft and matrix chains are described by plotting the probability distribution $P(R_{ee})$ of end-end distance R_{ee} . For each chain the R_{ee} is calculated as follows:

$$R_{ee} = \sqrt{|r_{i,l} - r_{i,1}|^2} \quad (3)$$

where $r_{i,1}$ and $r_{i,l}$ are the position vectors of the first and last beads of the ith graft or matrix chain.

I also calculate the free volume to quantify the unoccupied space surrounding each graft bead. I quantify the free volume of graft chains by using the method of Voronoi tessellation of space,³⁰ whereby the vectors joining each graft bead to all the other beads are perpendicularly bisected to obtain polyhedrons around each graft bead. Since the acceptor and donor beads in our model lie within parent graft and matrix beads and act merely as sites to facilitate hydrogen bonding between graft and matrix chains, they are excluded from the calculation of free volume. I note that this interpretation of free volume refers to the unoccupied volume around each graft bead and is measured by subtracting the occupied volume of the graft bead (i.e., the volume $\frac{4\pi r^3}{3}$ of a spherical bead of size $1d$) from the volume of the smallest polyhedron surrounding it. This calculation is performed by utilizing the open source library VORO++.³¹ The sum of free volumes of N_G graft beads that constitute a graft chain gives the effective free volume of a graft chain. I plot the probability distribution of free volume per graft chain from the ensemble of graft chains in all configurations in all three trials.

Chapter 2

SIMULATION RESULTS AND DISCUSSION

2.1 Results for Low Grafting Density Simulations

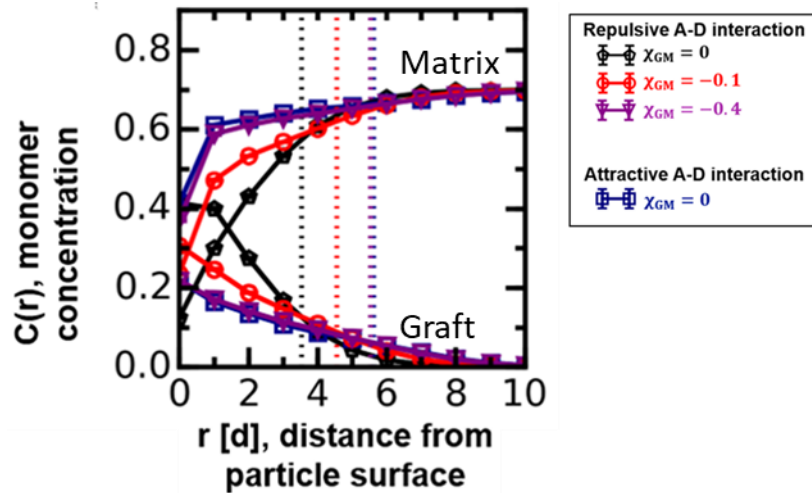


Figure 4 Graft (decreasing with distance from particle surface) and matrix (increasing with distance from particle surface) monomer concentration profiles for PNCs with isotropic graft-matrix interaction and repulsive A-D interaction and for PNCs with attractive A-D interaction. The dashed lines represent the brush height of the grafted layer. These results are for $D_P=5d$, $N_G=20$, $\Sigma=0.32$ chains/ d^2 and $N_M=20$. Error bars (calculated as standard deviation from three independent simulation runs) when not visible are smaller than marker size.

In Figure 4, I show the concentration of graft and matrix monomers as a function of distances from the nanoparticle surface. As distance from the particle surface increases, the concentration of graft monomers decreases. This is intuitive

because as one moves further from the particle surface, one would expect the likelihood of finding a graft monomer site to decrease. The matrix concentration profile lines indicate that there is some grafted layer wetting – where matrix monomers penetrate the layer of grafted monomers. Figure 4 shows that in the absence of attractive A-D interaction as χ_{GM} becomes progressively more negative, the grafted layer wetting increases due to the stronger enthalpic attraction. This figure also shows that a PNC with attractive A-D interaction of $\epsilon_{AD} = 13kT$ and $\chi_{GM} = 0$ has similar graft and matrix monomer concentration profiles as PNCs with isotropic $\chi_{GM} = -0.4$ in the absence of attractive A-D interaction. Table 1 is used to quantify more information about the wetting of the matrix into the grafted layer in these two systems to demonstrate the similarity between them.

Table 1: Quantification of grafted layer wetting for select systems, these results are for $D_P=5d$, $N_G=20$, $\Sigma =0.32$ chains/ d^2 and $N_M=20$.

Interactions	Average Number of matrix beads within grafted layer thickness (<i>dashed lines in concentration profiles</i>).
$\chi_{GM} = -0.4$, Repulsive A-D interactions.	1526.30 ± 2.78
$\chi_{GM} = 0$, Attractive A-D interactions.	1614.30 ± 1.25

I calculate the number of matrix beads within the grafted layer thickness to prove that the PNC with isotropic $\chi_{GM} = -0.4$ in the absence of attractive A-D

interaction has similar grafted layer wetting as the PNC with attractive A-D interaction of $\epsilon_{AD} = 13kT$ and $\chi_{GM} = 0$ (Table 1). This means that isotropic and anisotropic PNC interactions can achieve nearly equivalent wetting, but with an order of magnitude difference in strength of attraction; isotropic graft–matrix attraction $\epsilon_{GM} = 0.9kT$ that leads to $\chi_{GM} = -0.4$ achieves nearly equivalent wetting as directional A-D interaction of strength $\epsilon_{AD} = 13kT$. I hypothesize that equivalent wetting is achieved because the effective G-M interactions in both cases are equivalent. One could prove this hypothesis of equivalent effective G-M interactions by conducting computationally intensive potential of mean force calculations³² to quantify the $W_{GM}(r)$ for both systems. However, given the extensive simulation work that goes toward calculating these potentials of mean force, other members of the Jayaraman group have ongoing work to calculate the potential of mean forces through a theoretical approach.

One should note that the effective graft-matrix interaction will be influenced by the chosen graft-matrix attraction/repulsion, A-D interactions and entropic contributions from the PNC design (i.e., grafting density, particle size, graft and matrix chain lengths, and polymer grafted particle packing fraction in the matrix).

Now, after quantifying how the type of graft-matrix interaction (isotropic vs directional) impacts the structure of the grafted layer (the wetting/dewetting), we now will now investigate the effect of specific and directional attraction on the *individual chain conformations*.

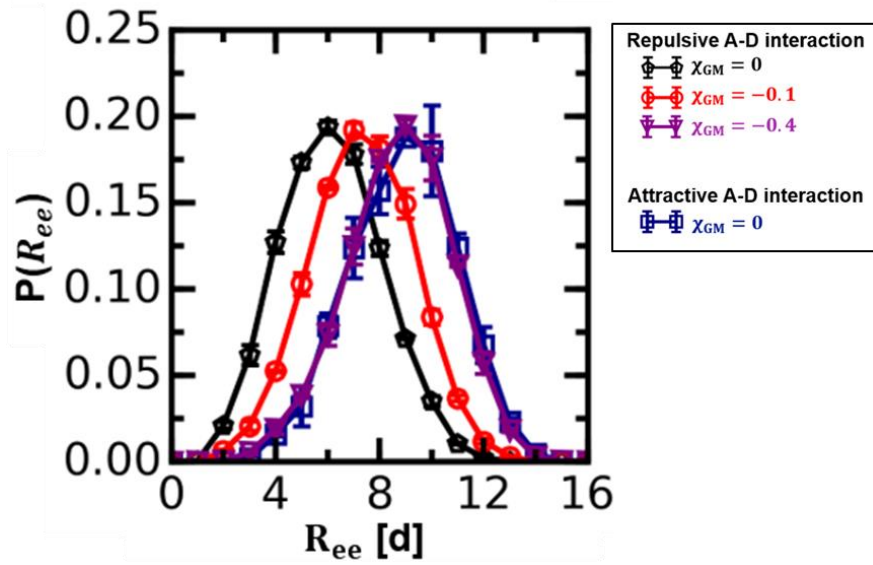


Figure 5: Probability distribution of the end-end distances, $P(R_{ee})$ vs. R_{ee} for graft chains. These results are for $D_P=5d$, $N_G=20$, $\Sigma=0.32$ chains/ d^2 and $N_M=20$. Error bars (calculated as standard deviation from three independent simulation runs) when not visible are smaller than marker size.

In Figure 5, I show the end-end distance of the graft chains under various strengths and mechanisms of attraction. As χ_{GM} decreases or directional attraction forces are introduced, the graft chains adopt more extended conformations corresponding to the increasing grafted layer wetting shown in Figure 4. Interestingly, the PNCs with equivalent wetting also have identical graft chain conformations, irrespective of whether the wetting was driven by isotropic G-M interactions or directional A-D interaction. This is likely true only for fully flexible graft chains considered here and may change as flexibility decreases. I do not show the matrix chain conformations in Figure 5 because at this low filler fraction the matrix chains in the grafted layer do not impact the matrix conformations in the bulk. One should note

that for each interaction case, the PNC with lower grafting density always exhibits significantly higher grafted layer wetting than its counterpart at the high grafting density discussed in the paper this thesis is adapted from.¹ This behavior is well known based on past literature cited in the introduction that decreasing grafting density should increase matrix penetration into the grafted layer. To quantify the extent to which A-D attractive interactions improve grafted layer wetting, I calculate the crossover point in the concentration profiles. This crossover point is defined as the value of r where $C(r)_{\text{graft}} = C(r)_{\text{matrix}}$. In Figure 4, the crossover point goes from $r = 1.45d$ to no crossover as one compares a PNC at the purely entropic limit to a PNC with directional A-D attraction (i.e., going from the black line to navy blue line). The shift in crossover point shows an increase in grafted layer wetting due to A-D attraction, but the shift is small for the PNCs at this low grafting density because the grafted layer is significantly wet even at the purely entropic limit.

Thus far, we have observed that it is possible to get equivalent wetting and chain conformations with hydrogen bonding or isotropic attractions. Therefore, this raises the question, what makes the specific and directional interactions present in these systems unique? One may expect that the nature of these interactions may lead to fewer and tighter contacts between graft and matrix (hydrogen bonding is usually short ranged). Therefore, in Table 2, the number of matrix chains experiencing attractive enthalpic forces with each graft chain is shown. In Figure 6, the free volume per graft chain is shown.

Table 2: Number of matrix chains interacting with each graft chain for the two cases of equivalent wetting. These results are for $D_P=5d$, $N_G=20$, $\Sigma =0.32$ chains/ d^2 and $N_M=20$.

Interactions	Average number of matrix chains interacting with each graft chain.
$\chi_{GM} = -0.4$, Repulsive A-D interactions.	25.52 ± 0.16
$\chi_{GM} = 0$, Attractive A-D interactions.	11.39 ± 0.16

In the case of attraction created via directional A-D interactions, each graft chain interacts with 11.39 ± 0.16 matrix chains. In contrast, when the attraction is created via isotropic G-M interactions ($\chi_{GM} = -0.4$) each graft interacts with 25.52 ± 0.16 matrix chains. This indicates, that while the strength of the acceptor donor attraction is much stronger (13kT vs 0.9 kT), the specificity and short ranged nature lead to fewer matrix chains able to experience this potential energy well.

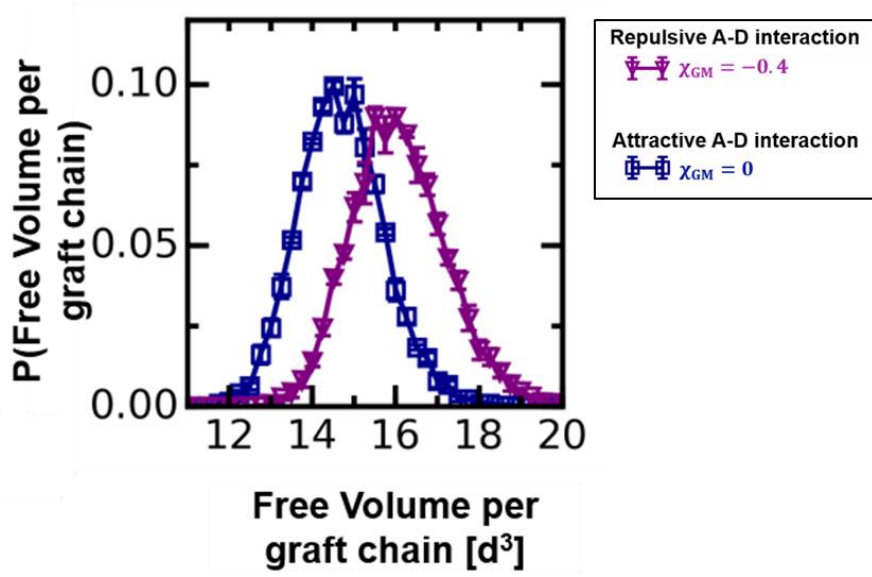


Figure 6: Probability distribution of free volume per graft chain for the two cases that show equivalent wetting in Figure 4 and equivalent end-end distances in Figure 5. These results are for $D_p=5d$, $N_G=20$, $\Sigma=0.32$ chains/ d^2 and $N_M=20$. Error bars (calculated as standard deviation from three independent simulation runs) when not visible are smaller than marker size.

Interestingly, despite the graft chains interacting with fewer matrix chains in the case of attractive A-D interactions, the free volume for each graft chain (Figure 6) is lower for PNCs with directional A-D interaction as compared to the PNC with isotropic G-M attraction. This means that even though structurally the wetting (i.e., net interpenetration of the graft and matrix chains) is the same, and the graft and matrix conformations are also similar, the graft and matrix contact is “tighter” in the case of PNCs with H-bonding interaction as compared to PNCs with isotropic G-M attraction or $\chi_{GM} < 0$.

2.2 CONCLUSIONS AND FUTURE WORK

In this thesis I present a new coarse-grained (CG) polymer model that captures specific and directional hydrogen bonding interactions between the graft and matrix polymers for PNCs comprised of polymer grafted nanoparticle placed in a polymer matrix. Using this CG model, I show the impact of introducing hydrogen bonding chemistries in the graft and matrix polymers on the grafted layer wetting, grafted chain conformations, and the free volume in the grafted layer. Our results show that directionally attractive interactions between graft and matrix chains improve the grafted layer wetting over purely entropically driven PNCs similar to isotropic attractions. The grafted chains extend towards the matrix chains to make acceptor-donor contacts thereby increasing the grafted layer thickness and increasing the interpenetration of matrix chains into the grafted layer. Comparison of PNCs with isotropic graft-matrix interactions and PNCs with directional hydrogen bonding type interactions between graft and matrix chains shows that one can achieve equivalent wetting (as seen by overlapping monomer concentration profiles, graft conformations and number of matrix beads within grafted layer) with the directional hydrogen bonding interaction strength that is an order of magnitude larger than the isotropic graft-matrix attraction strength. Interestingly, despite equivalent wetting and grafted chain conformations, I find that PNCs with directional hydrogen bonding type interactions between graft and matrix chains have a lower free volume per graft chain than PNCs with isotropic graft-matrix interaction. This suggests that directional acceptor-donor interactions induce a tighter graft-matrix contact in PNCs. The paper this thesis references also finds the above trends to hold both at the high and low grafting density regimes as well as matrix chain length/graft chain length ratio of 3 and 1.¹ These results suggest that incorporating hydrogen bonding between graft and

matrix monomers can be an effective means for improving grafted layer wetting and as a result, increasing particle dispersion in PNCs. At the same time, the thermomechanical properties of PNCs with hydrogen interactions between graft and matrix monomers may be different from another PNC that has isotropic graft-matrix interactions and an identical grafted layer wetting.

In terms of future directions, one can use this CG model for other hydrogen bonding polymeric systems beyond PNCs, like polymer blends, block copolymer mixtures, etc. Even though the focus of this thesis is on structural features like grafted layer wetting, graft and matrix chain conformations and free volume, there are ongoing efforts in our group to evaluate how well this CG model captures dynamic information both at the small timescale of h-bonding (e.g., hydrogen bond lifetimes) and long timescale of polymer relaxation.

REFERENCES

1. Kulshreshtha, A.; Modica, K. J.; Jayaraman, A. Impact of Hydrogen Bonding Interactions on Graft–Matrix Wetting and Structure in Polymer Nanocomposites. *Macromolecules* 2019, 52, 2725-2735.
2. Ganesan, V.; Jayaraman, A. Theory and simulation studies of effective interactions, phase behavior and morphology in polymer nanocomposites. *Soft matter* 2014, 10, 13-38.
3. Arthi Jayaraman Polymer grafted nanoparticles: Effect of chemical and physical heterogeneity in polymer grafts on particle assembly and dispersion. *Journal of Polymer Science. Part B, Polymer Physics* 2013, 51, 524-534.
4. Jancar, J.; Douglas, J. F.; Starr, F. W.; Kumar, S. K.; Cassagnau, P.; Lesser, A. J.; Sternstein, S. S.; Buehler, M. J. Current issues in research on structure–property relationships in polymer nanocomposites. *Polymer* 2010, 51, 3321-3343.
5. Hall, L. M.; Jayaraman, A.; Schweizer, K. S. Molecular theories of polymer nanocomposites. *Current Opinion in Solid State & Materials Science* 2010, 14, 38-48.
6. Krishnamoorti, R.; Vaia, R. A. Polymer nanocomposites. *Journal of Polymer Science Part B: Polymer Physics* 2007, 45, 3252-3256.
7. Modica, K. J.; Martin, T. B.; Jayaraman, A. Effect of Polymer Architecture on the Structure and Interactions of Polymer Grafted Particles: Theory and Simulations. *Macromolecules* 2017, 50, 4854-4866.
8. Martin, T. B.; Mongcopa, K. I. S.; Ashkar, R.; Butler, P.; Krishnamoorti, R.; Jayaraman, A. Wetting–Dewetting and Dispersion–Aggregation Transitions Are Distinct for Polymer Grafted Nanoparticles in Chemically Dissimilar Polymer Matrix. *Journal of the American Chemical Society* 2015, 137, 10624-10631.

9. Heo, K.; Miesch, C.; Emrick, T.; Hayward, R. C. Thermally Reversible Aggregation of Gold Nanoparticles in Polymer Nanocomposites through Hydrogen Bonding. *Nano letters* 2013, 13, 5297-5302.
10. Rasheed, A.; Chae, H. G.; Kumar, S.; Dadmun, M. D. Polymer nanotube nanocomposites: Correlating intermolecular interaction to ultimate properties. *Polymer* 2006, 47, 4734-4741.
11. Moskala, E. J.; Howe, S. E.; Painter, P. C.; Coleman, M. M. On the role of intermolecular hydrogen bonding in miscible polymer blends. *Macromolecules* 1984, 17, 1671-1678.
12. Viswanathan, S.; Dadmun, M. D. Guidelines To Creating a True Molecular Composite: Inducing Miscibility in Blends by Optimizing Intermolecular Hydrogen Bonding. *Macromolecules* 2002, 35, 5049-5060.
13. Kuo, S.; Lin, C.; Chang, F. The study of hydrogen bonding and miscibility in poly(vinylpyridines) with phenolic resin. *Polymer* 2002, 43, 3943-3949.
14. Eichhorn, K.; Fahmi, A.; Adam, G.; Stamm, M. Temperature-dependent FTIR spectroscopic studies of hydrogen bonding of the copolymer poly(styrene- b-4-vinylpyridine) with pentadecylphenol. *Journal of Molecular Structure* 2003, 661, 161-170.
15. Yusa, S.; Sakakibara, A.; Yamamoto, T.; Morishima, Y. Fluorescence Studies of pH-Responsive Unimolecular Micelles Formed from Amphiphilic Polysulfonates Possessing Long-Chain Alkyl Carboxyl Pendants. *Macromolecules* 2002, 35, 10182-10188.
16. Coleman, M. M.; Serman, C. J.; Bhagwagar, D. E.; Painter, P. C. A practical guide to polymer miscibility. *Polymer* 1990, 31, 1187-1203.
17. Starr, F. W.; Sciortino, F. Model for assembly and gelation of four-armed DNA dendrimers. *Journal of Physics: Condensed Matter* 2006, 18, L353.
18. Largo, J.; Starr, F. W.; Sciortino, F. Self-Assembling DNA Dendrimers: A Numerical Study. *Langmuir : the ACS journal of surfaces and colloids* 2007, 23, 5896-5905.
19. Ghobadi, A. F.; Jayaraman, A. Effect of backbone chemistry on hybridization thermodynamics of oligonucleic acids: a coarse-grained molecular dynamics simulation study. *Soft matter* 2016, 12, 2276-2287.

20. Condon, J. E.; Jayaraman, A. Development of a Coarse-Grained Model of Collagen-Like Peptide (CLP) for Studies of CLP Triple Helix Melting. *The journal of physical chemistry. B* 2018, 122, 1929-1939.
21. Prhashanna, A.; Taylor, P. A.; Qin, J.; Kiick, K. L.; Jayaraman, A. Effect of Peptide Sequence on the LCST-Like Transition of Elastin-Like Peptides and Elastin-Like Peptide-Collagen-Like Peptide Conjugates: Simulations and Experiments. *Biomacromolecules* 2019, 20, 1178-1189.
22. Grest, G.; Kremer, K. Molecular dynamics simulation for polymers in the presence of a heat bath. *Physical review. A, General physics* 1986, 33, 3628-3631.
23. Lin, B.; Martin, T. B.; Jayaraman, A. Decreasing Polymer Flexibility Improves Wetting and Dispersion of Polymer-Grafted Particles in a Chemically Identical Polymer Matrix. *ACS Macro Letters* 2014, 3, 628-632.
24. Jones, J. E. On the Determination of Molecular Fields. II. From the Equation of State of a Gas. *Proceedings of the Royal Society A: Mathematical, Physical and Engineering Sciences* 1924, 106, 463-477.
25. Kuo, S. Hydrogen-bonding in polymer blends. *J Polym Res* 2008, 15, 459-486.
26. Weeks, J. D.; Chandler, D.; Andersen, H. C. Role of Repulsive Forces in Determining the Equilibrium Structure of Simple Liquids. *The Journal of Chemical Physics* 1971, 54, 5237-5247.
27. Plimpton, S. Fast Parallel Algorithms for Short-Range Molecular Dynamics. *Journal of Computational Physics* 1995, 117, 1-19.
28. Stukowski, A. Visualization and analysis of atomistic simulation data with OVITO—the Open Visualization Tool. *Modelling and Simulation in Materials Science and Engineering* 2010, 18, 015012.
29. Dammert, R. M.; Maunu, S. L.; Maurer, F. H. J.; Neelov, I. M.; Niemelä, S.; Sundholm, F.; Wästlund, C. Free Volume and Tacticity in Polystyrenes. *Macromolecules* 1999, 32, 1930-1938.
30. Rycroft, C. H. VORO++: A three-dimensional Voronoi cell library in C++. *Chaos: An Interdisciplinary Journal of Nonlinear Science* 2009, 19, 1.

31. Smith, G. D.; Bedrov, D. Dispersing Nanoparticles in a Polymer Matrix: Are Long, Dense Polymer Tethers Really Necessary? *Langmuir : the ACS journal of surfaces and colloids* 2009, 25, 11239-11243.

Appendix

TEXT AND FIGURE REPRINT PERMISSION

**Copyright Clearance Center**

**RightsLink[®]**

[Home](#) [Create Account](#) [Help](#) 

**ACS Publications** Most Trusted. Most Cited. Most Read.

Title: Impact of Hydrogen Bonding Interactions on Graft-Matrix Wetting and Structure in Polymer Nanocomposites

Author: Arjita Kulshreshtha, Kevin J. Modica, Arthi Jayaraman

Publication: Macromolecules

Publisher: American Chemical Society

Date: Apr 1, 2019
Copyright © 2019, American Chemical Society

LOGIN
If you're a [copyright.com](#) user, you can login to RightsLink using your [copyright.com](#) credentials. Already a RightsLink user or want to [learn more?](#)

PERMISSION/LICENSE IS GRANTED FOR YOUR ORDER AT NO CHARGE

This type of permission/license, instead of the standard Terms & Conditions, is sent to you because no fee is being charged for your order. Please note the following:

- Permission is granted for your request in both print and electronic formats, and translations.
- If figures and/or tables were requested, they may be adapted or used in part.
- Please print this page for your records and send a copy of it to your publisher/graduate school.
- Appropriate credit for the requested material should be given as follows: "Reprinted (adapted) with permission from (COMPLETE REFERENCE CITATION). Copyright (YEAR) American Chemical Society." Insert appropriate information in place of the capitalized words.
- One-time permission is granted only for the use specified in your request. No additional uses are granted (such as derivative works or other editions). For any other uses, please submit a new request.

[BACK](#)[CLOSE WINDOW](#)

Copyright © 2019 [Copyright Clearance Center, Inc.](#) All Rights Reserved. [Privacy statement](#). [Terms and Conditions](#).
Comments? We would like to hear from you. E-mail us at customercare@copyright.com